

Article

# Assessment of Compressive Sensing $2 \times 2$ MIMO Antenna Design for Millimeter-Wave Radar Image Enhancement

Neda Rojhani , Marco Passafiume , Matteo Lucarelli , Giovanni Collodi  and Alessandro Cidronali 

Department of Information Engineering, University of Florence, via Santa Marta, 3, 50139 Firenze, Italy; marco.passafiume@unifi.it (M.P.); matteo.lucarelli@unifi.it (M.L.); giovanni.collodi@unifi.it (G.C.); alessandro.cidronali@unifi.it (A.C.)

\* Correspondence: neda.rojhani@unifi.it

Received: 11 March 2020; Accepted: 3 April 2020; Published: 9 April 2020



**Abstract:** This paper presents a microstrip array antenna designed for a  $2 \times 2$  Compressive Sensing Multiple-Input Multiple-Output (CS-MIMO) millimeter-wave radar operating at 37.5 GHz. The CS-MIMO linear array antenna is designed to obtain an optimal aperture by seeking a suitable random pattern for the antenna positions. Applying CS allows a considerable reduction in the number of antennas respect to a dense array based on the Nyquist criterion. In this study, we report all possible configurations of  $2 \times 2$  CS-MIMO by placing antennas in random positions, plus their compression ratio. Finally, by selecting the proper design, we examine the experimental validation of the CS-MIMO antenna prototype by comparing measurements and simulations with a Standard MIMO (Std-MIMO) antenna prototype as a benchmark. The experimental results show that the angular resolution can be increased through a random array CS-MIMO by a factor of at least 2.9 respect to Std-MIMO while preserving the radar field of view.

**Keywords:** Multiple-Input Multiple-Output Radar; Compressive Sensing (CS); millimeter-wave antenna

## 1. Introduction

In radar systems technology one of the main constraints is represented by the cross-range resolution, which is the radar capability to resolve targets at the same range but placed at different angles. This capability is obviously dominated by the radar angular resolution. For co-located radar systems, increasing the antenna aperture is a straightforward approach to improve the corresponding system performance [1]. However, increasing the number of elements in the antenna array raises the overall dimensions of the device and the complexity of the radar front-end.

More recently, the adoption of specific transmitted signal waveforms has been considered as a viable approach to improve angular resolution, while limiting the number of antenna elements. This approach resulted in the development of Multiple-Input Multiple-Output (MIMO) radars [2,3]. The basic concept of MIMO radar systems relies on the capability to transmit mutually orthogonal signals from multiple transmitting antennas, thus generating multiple orthogonal received signals [4]. This feature enhances target detection [5], and allows higher angular resolution [6], when compared to conventional radars of comparable complexity. Given this, the MIMO technique has been largely investigated and successfully adopted in many applications, also for automotive radar systems [1,7], and in particular in the millimeter-wave frequency range [8].

In standard MIMO (Std-MIMO) radars, the combination of  $M$ -elements spaced by  $\frac{\lambda}{2}$  in receiving/transmitting, and  $N$ -elements spaced by  $M\frac{\lambda}{2}$  in transmission/reception is equivalent

to a Uniform Linear Array (ULA) comprised of  $M \times N$  virtual antennas. Note that the Nyquist configuration, as this standard arrangement is also called, suffers one drawback: the product of transmitter and receiver antennas,  $M \times N$ , requires a linearly scaled array aperture for a specific resolution. Consequently, while the use of millimeter-wave frequency band helps in keeping limited the physical dimension of the radar front-end, high angular resolution requires a high number of radar transceiver channels, thus making complex and expensive the development of high angular resolution radar systems in any practical case.

To address this limitation, MIMO radars have been investigated further by exploiting the Compressive Sensing (CS) technique [9]. Applying the CS to a MIMO radar [10], allows using random antenna positions in a larger aperture with respect to the Std-MIMO radar. It means that the spatial CS obtains an angular resolution similar to or better than the field array antennas based on the Nyquist criterion, with a significant reduction of the number of antennas. Lowering the Nyquist rate spatial sampling translates into fewer transceiver channels and thus comparably lower system complexity. Nevertheless, CS requires a minimum quantity of elements in order to obtain a meaningful quantity of information to guarantee correct targets recovery. Determining the exact conditions that assure a proper recovery has been a main topic of research on CS. Results have shown that, there exist a minimum number of independent and non-uniform sensing measurements needed for meaningful CS applications [11]. Although the CS technique has a sufficiently strong theoretical basis, its effective implementation in real applications still needs experimentation and validations. This is particularly true for millimeter-wave frequency band applications, where the experimental implementations are still in a preliminary stage [12,13]. On this basis, the authors have investigated the possible random distributions for the antenna array elements that are suitable for the correct CS technique applied to a millimeter-wave MIMO radar, as well as its effective impact on radar angular resolution, also in comparison with a similar standard MIMO device.

Specifically, the contributions of this work are the following: firstly, we assess all the possible configurations of the  $2 \times 2$  CS-MIMO with respect to their compression ratio and expected angular resolution. Secondly, on this basis, we present the performance comparison between a 37.5 GHz patch array antenna prototype for a  $2 \times 2$  CS-MIMO radar, which was developed according to our assess, and a corresponding Std-MIMO antenna.

For the first time, in this paper, we validate experimentally that angular resolution can be improved using a properly designed CS-MIMO array by a factor of at least 2.9 with respect to Std-MIMO, while maintaining the field of view of radar.

This paper is organized as it follows. In Section 2, we report the basic theory of the CS and the description of all the possible antenna configurations of a  $2 \times 2$  CS-MIMO; the configurations are compared by proper figure of merit. Section 3 describes the antenna design, along with the radar measurement laboratory set-up. Finally, in Section 4 we discuss the experimental results that validate the effective exploitation of the CS technique for millimeter-wave MIMO radar.

## 2. CS-MIMO Antenna Configuration Assessment

The most straightforward Std-MIMO array configuration provides  $N_{RX} \cdot N_{TX}$  possible independent positions to be synthesized using  $N_{RX}$  receiving antenna, with the inter-element physical spacing  $d_{RX} = \frac{\lambda}{2}$ , arranged side by side to  $N_{TX}$  transmitting antennas, with an inter-element physical spacing of  $d_{TX} = N_{RX} \cdot d_{RX}$ . Basically, when one  $TX$  antenna, in the  $p_{TX}$  position, and one  $RX$  antenna, in the  $p_{RX}$  position, are both switched on, and the others are switched off, they are equivalent to one single *virtual antenna* placed at the median point  $\frac{(p_{TX}+p_{RX})}{2}$ . This topology states that given the Nyquist theorem requirement, the spatial step between virtual antennas should be equal to a quarter of wavelength, i.e.,  $d = \frac{\lambda}{4}$ , for omnidirectional antennas [14], and leads to maximum equivalent antenna aperture  $L_e = (N_{RX} \cdot N_{TX} - 1) d$ .

According to the CS technique, a signal of interest  $\mathbf{x} \in R^{N \times 1}$ , which is assumed to be sparse in the range-angle space, can be recovered with far fewer samples than needed by Nyquist theory or

equivalent from the measurement vector,  $\mathbf{y} \in R^{M \times 1}$  [9,15]. Hence, we expect that the same  $L_e$  could be achieved with fewer elements than  $N_{RX} + N_{TX}$ , with regards to the conventional MIMO configuration. Worth mentioning that the CS relies on two fundamental requirements: sparsity and incoherency [16]. Although the radar signal typically has intrinsic sparsity property, providing the second requirement is not easy because it depends on the sensing matrix [9]. In the sensing matrix selection process, there is a degree of freedom represented by the  $TX/RX$  antenna positions which are provided by the measurement vector  $\mathbf{y}$  [11,17]. Therefore, their arrangement is crucial in CS-MIMO antenna design because exploiting the random sampling of antennas that are placed over a large aperture allows a significant reduction in the number of antennas needed to achieve similar or better resolution of a dense (Nyquist) array. In addition, by leveraging of random sampling positions, we fulfill the incoherency requirement.

Let us recall the goal of this investigation is to assess the expected performance of a MIMO antenna configuration designed by the CS technique, and the consequent selection of a proper configuration capable of providing enhanced angular resolution with respect to the standard dense configuration, and validate the choice experimentally at millimeter-wave frequencies.

The performance of each specific CS configuration is assessed by its Compression Ratio,  $CR$ , defined as the ratio between the number of virtual antennas available in the  $L_e$  associated to the Std-MIMO, and the equivalent number of virtual antennas existing in the CS-MIMO aperture,  $L_e^{CS}$ . It is worth mentioning that in the latter, the number of virtual antennas is obtained by taking into account the total positions of the CS-MIMO aperture.

$$CR = 100 \frac{(N_{RX} \cdot N_{TX})_{L_e}}{(N_{RX} \cdot N_{TX})_{L_e^{CS}}} \quad (1)$$

For instance, a  $CR$  of 50% corresponds to the  $2 \times 2 = 4$  antennas providing non-zero signals, and randomly selected among 8 virtual antennas uniformly spaced of  $\frac{\lambda}{4}$  in CS-MIMO. Consequently, the angular resolution,  $(\Delta\theta)$ , is given by:

$$\Delta\theta = \frac{\lambda}{2L_e^{CS} \cos\theta} \quad (2)$$

where  $\theta$  is the angle of arrival with respect to the radar, and  $L_e^{CS}$  is the equivalent antenna aperture of the CS-MIMO.

Since incoherency and sparsity of the radar signal require to sample at least 30–40% of the data available based on the Nyquist theorem, we considered the  $CR = 40\%$ , as the best trade-off between  $CR$  and signal quality; according to the CS optimization results reported in [14].

In this work, we consider the set of possible antenna arrangements composed of  $N_{TX} = 2$  and  $N_{RX} = 2$ , distributed in a linear grid uniformly spaced with step  $\frac{\lambda}{4}$ , with a total of 21 available positions, i.e., maximum aperture  $5\lambda$ . This aperture length has been chosen due to the limitations of in-house antenna printing process. All available configurations are listed in Table 1, which reports the place of receiving antenna  $RX_1$  in position #1 and the transmitting antenna  $TX_1$  in position #21 for all possible arrangements, while the remaining  $TX/RX$  antennas are randomly placed in a large aperture along 11 notches at step  $\frac{\lambda}{2}$ . All practical arrangements are equivalent to 72 configurations. It is noteworthy that 8 of them have to be rejected having duplicate locations for the virtual antennas. From the data reported in Table 1 we can observe a proportional increase of resolution at  $\theta = 0 \text{ deg}$  as the  $CR$  reduces.

Figure 1 shows a specific case based on  $CR = 40\%$ , when the receiving antenna  $RX_1$  is placed in position #1 of the linear grid, while the transmitting antenna  $TX_1$  is placed in position #21 of the same grid, and the  $RX_2$  in position #3 and  $TX_2$  in position #5; the resulting virtual antennas are placed in positions #3, #4, #11, and #12, which are 4 out of the 10 total positions, and refers to the center point

between each TX/RX antenna. In other words, using CR equal to 40% will be equivalent to 10 virtual antennas but using only 4 physical centers of phase.

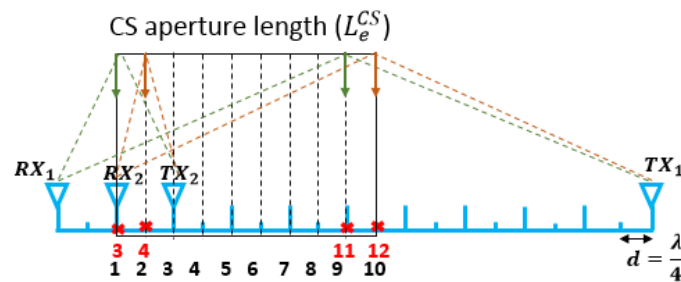


**Figure 1.** Schematic representation of the CS-MIMO antenna configuration. Crosses represent the positions of virtual antennas; black numbers on grid refer to the CS aperture, red numbers to physical positions.

**Table 1.** TX<sub>2</sub>/RX<sub>2</sub> antennas positions along with their CR when RX<sub>1</sub> is in position #1, and TX<sub>1</sub> is in position #21. The bold one corresponds to the developed prototype configuration.

Rx <sub>2</sub>	Tx <sub>2</sub>	CR	Δθ	Rx <sub>2</sub>	Tx <sub>2</sub>	CR	Δθ	Rx <sub>2</sub>	Tx <sub>2</sub>	CR	Δθ
3	19	reject	—	9	19	67%	23°	15	19	44%	14.3°
3	17	100%	38°	9	17	57%	19°	15	17	40%	12.7°
3	15	80%	28°	9	15	50%	16.4°	15	13	33%	11.4°
3	13	67%	23°	9	13	reject	—	15	11	30%	9.5°
3	11	57%	19°	9	11	40%	12.7°	15	9	28%	8.8°
3	9	50%	16.4°	9	7	33%	11.4°	15	7	reject	—
3	7	44%	14.3°	9	5	30%	9.5°	15	5	25%	7.6°
3	5	<b>40%</b>	<b>12.7°</b>	9	3	28%	8.8°	15	3	23%	7.2°
5	19	100%	38°	11	19	57%	19°	17	19	40%	12.7°
5	17	reject	—	11	17	50%	16.37°	17	15	33%	11.4°
5	15	67%	23°	11	15	44%	14.33°	17	13	30%	9.5°
5	13	57%	19°	11	13	40%	12.7°	17	11	28%	8.8°
5	11	50%	16.4°	11	9	33%	11.4°	17	9	26%	8.2°
5	9	44%	14.3°	11	7	30%	9.5°	17	7	25%	7.6°
5	7	40%	12.7°	11	5	28%	8.8°	17	5	reject	—
5	3	33%	11.4°	11	3	26%	8.2°	17	3	22%	6.7°
7	19	80%	28°	13	19	50%	16.37°	19	17	33%	11.4°
7	17	67%	23°	13	17	44%	14.33°	19	15	30%	9.5°
7	15	reject	—	13	15	40%	12.7°	19	13	28%	8.8°
7	13	50%	16.37°	13	11	33%	11.4°	19	11	26%	8.2°
7	11	44%	14.33°	13	9	reject	—	19	9	25%	7.6°
7	9	40%	12.7°	13	7	28%	8.8°	19	7	23%	7.2°
7	5	33%	11.4°	13	5	26%	8.2°	19	5	22%	6.7°
7	3	30%	9.5°	13	3	25%	7.6°	19	3	reject	—

The antenna topologies reported in Table 1 have been considered to simulate the MIMO radar response with respect to an ideal target; the simulations assume that the radar operates a FMCW waveform with 1.5 GHz bandwidth around 37.5 GHz, while the signal reconstruction was carried out using the Fast Fourier Transformation (FFT) as basis matrix and Orthogonal Matching Pursuit Algorithm (OMP) as a recovery technique. After reconstruction, the data has been focused according to the phase history of each contribution corresponding to a particular one frequency and position with a back-projection technique. Figure 2a shows the results of the simulations in terms of angular power plot for the cases reported in Table 1, which confirms the inverse dependence of the improved angular resolution with the CR reduction. The case CR = 100% corresponds to standard MIMO topology. It is noteworthy, that multiple TX/RX antenna positions lead to the same compression. Figure 2b demonstrates that in 8 different antenna combinations, for which the compression is equal to 40%, the resolution remains the same.

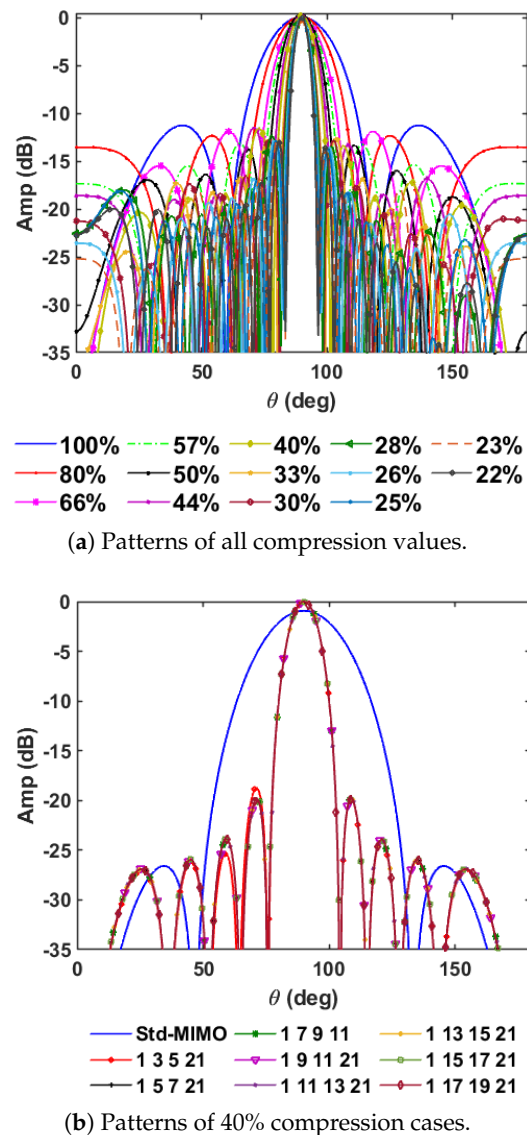


**Figure 2.** Simulated normalized power plots of a target in front of the MIMO radar for the cases reported in Table 1.

### 3. The CS-MIMO Radar

#### 3.1. CS-MIMO Antenna Prototype Design

The single element of the MIMO array was designed as a serially fed linear patch antenna array configuration [18], operating at the center frequency of 37.5 GHz. The array is composed of six linear polarized rectangular patches designed following standard patch design rules [19–21]. These series transmission lines not only connect each patch to the next one, but by properly allocating amplitude and phase of the signal in each patch also favor impedance matching to assist reaching a maximum level of versatility. The main reason for this outline is to provide a convenient antenna configuration, suitable for edge board connections to the TX and RX radar front-end channels.

To attain the desired bandwidth and maximum gain, the geometrical parameters of each element and their interconnecting transmission lines were optimized using an electromagnetic full-wave analysis engine, with the goal to optimize phase and amplitude feeding among the patches. Therefore, the patch dimensions and mutual distances are the parameters that maximally optimize the antenna performance. The dimensions are equal to  $3 \times 1.87 \text{ mm}^2$  for the first patch stage and  $3 \times 2.2 \text{ mm}^2$  for the others, while the inter-element distance is approximately equal to half of the wavelength.

The prototype has been realized on a 12 mil plastic laminate, Isola-Astra MT77 (thickness = 0.3175 mm,  $\epsilon_r = 3.02$ ,  $\tan\delta = 0.0017$ ), and its picture is shown in Figure 3a. A comparison between the simulated and measured antenna gain at center frequency and in vertical polarization is reported in Figure 3b. While the simulation predicts a maximum gain at  $\theta = 0\text{ deg}$  of 12.2 dB, experimental data reports a realized gain of 10.0 dB in the bandwidth 36.75–38.25 GHz, with a return loss better than 10 dB in the same bandwidth. This data is consistent with the measurement set up uncertainty of  $\pm 2\text{ dB}$ .

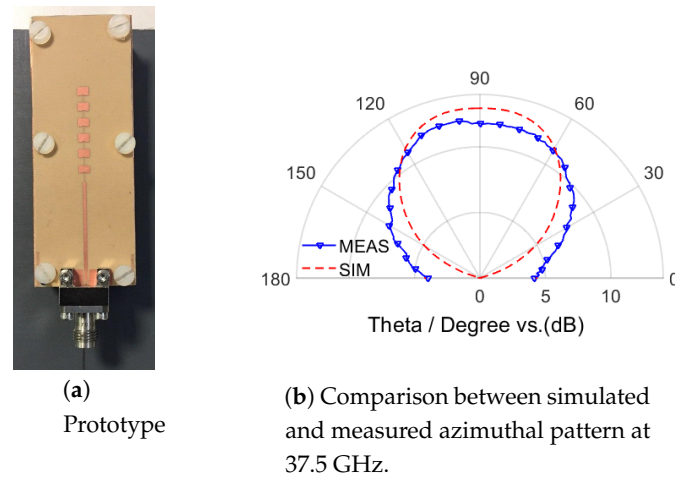


Figure 3. Single element antenna.

The single element prototype discussed herein-above was utilized to develop the two MIMO antennas adopted in this work. The first consists in the standard  $2 \times 2$  MIMO antenna prototype, shown in Figure 4a, whose antenna displacement respects the standard design technique, i.e., with spacing between RX antennas equal to  $\lambda/2$ , and spacing between TX antennas equal to  $\lambda$ ; the two set of antennas are displaced by  $\lambda$ . The second prototype was arranged by the CS-MIMO technique discussed in Section 2. It has the same single antenna elements in position:  $RX_1$ : #1,  $RX_2$ : #3,  $TX_1$ : #21, and  $TX_2$ : #5. A picture of this second prototype is shown in Figure 4b. The antenna prototypes were completed with a metallic carrier, which provides mechanical strength, and 2.4 mm edge launch coaxial connectors.

It is worth mentioning that for these MIMO configurations, in case of tight requirements in terms of range performance, a strategy to reduce the transmitter to receiver induced noise, consists in either using a signal source with superior phase noise characteristics or in decreasing the magnitude of the transmitter leakage signal; the latter can be obtained by using proper adaptive leakage power cancellation techniques, like those described in [22,23].

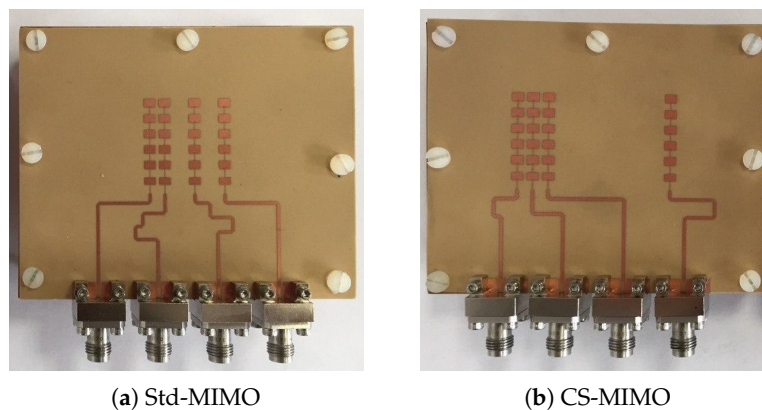


Figure 4. Photograph of  $2 \times 2$  MIMO antenna prototype assemblies.

### 3.2. Experimental MIMO Radar Measurement Set-Up

The conceptual MIMO radar system was implemented by using laboratory and test equipments in a controlled anechoic environment of dimensions  $4.9 \times 7 \text{ m}^2$ . The set-up permits to estimate the antenna characteristics, maintaining under control all the experimental radar parameters that may affect the experiment and thus the validation of the study. The schematic representation of the laboratory measurement set-up is reported in Figure 5a, while in Figure 5a is presented a picture of the laboratory set-up, where the absorbing panels spread throughout the floor and the walls are visible. For the purpose of a quantitative characterization, a 4-channels Vector Network Analyzer (VNA) operated as the radar transceiver front-end, and provided the required transmitting FMCW signals and the corresponding received signals suitable for off-line post-processing. A set of phase-stable coaxial cables connect the 4-ports VNA to the connectors of the array antenna prototype under test, with the latter placed on a rotary stand. The VNA was full-port calibrated at the antenna connectors section in the following band:  $f_{min} = 36.75 \text{ GHz}$ ,  $f_{max} = 38.25 \text{ GHz}$ , with a number of points equal to  $N_f = 3201$ . Because of the VNA wide dynamic range, and the assumption of a coherent channel, the radar signal process is suitable for the quantitative comparison of the two antenna prototypes. The radar target is a single non-ideal corner reflector of 0.2 m diameter placed at 3.25 m from the antenna prototype, and is shown in Figure 5b.

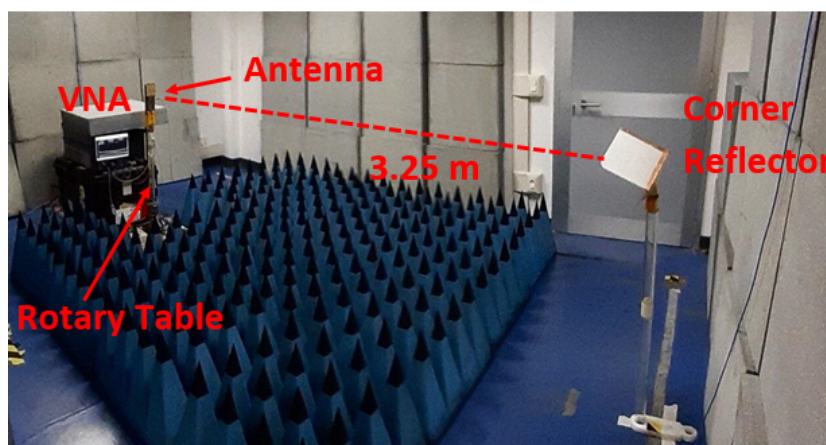
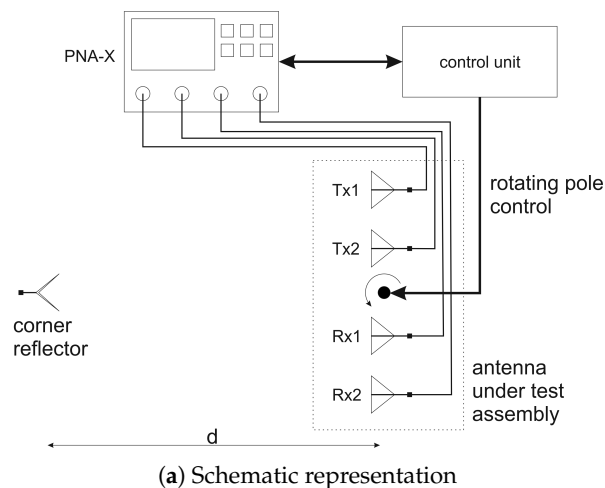


Figure 5. Experimental validation of the antenna sets in the laboratory set-up.

#### 4. Experimental Validation

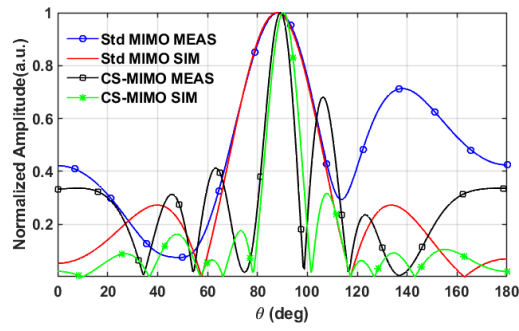
In this section, we examine and discuss the MIMO prototypes with aim to validate the performance of the proposed CS-MIMO antenna topology; all the experimental data were obtained with the antenna design and assessment technique described in Section 2.

To achieve this, Figure 6 compares the cuts of the radar images at the range distance of 3.25 m for the two MIMO prototypes; the data were normalized with respect to their maximum to allow a direct comparison. Since the CS performance depends drastically on the target angular position, the experiment was performed by assuming the corner reflector placed at different viewing angles, namely at  $\theta = 0, 12$  and  $24 \text{ deg}$ ; in other words, the 4-channels measurement acquisition of the 16 S-parameters set has been repeated for each angle of rotation of the rotary stand, and stored for further processing. Because the S-parameters are acquired simultaneously, we can assume that they represent a consistent set of data for the processing of the radar image at each step. The absence of any other interference, either electromagnetic or mechanical, made us reasonably sure about the fact that the data could be assumed coherent also through the entire range of observation angle. In addition, a measurement without the target has been carried out for each angle for clutter removal.

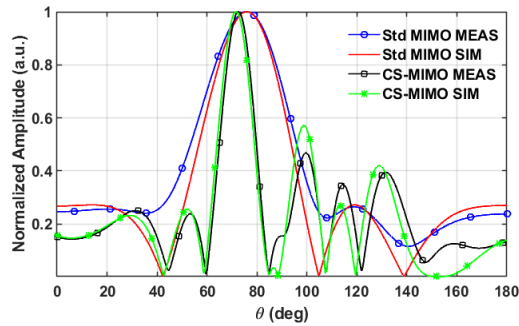
Simulations were performed by running a MATLAB code replicating the MIMO radar, which considers for each linear array the measured radiation pattern shown in Figure 3. These simulations assume ideal corner reflector positions at the proper angle of view, and don't consider any coupling and perturbation effects between antennas or non-ideal shape of corner reflector.

For both simulated and measured data, the signal reconstruction was carried out using the FFT as a basis matrix and OMP as a recovery technique, while the data has been focused via a back-projection technique, as mentioned before. We can observe that the angular resolutions are in agreement with the expected values provided in Table 1; namely, their estimations are  $\Delta\theta = 12.5 \text{ deg}$  and  $\Delta\theta = 37 \text{ deg}$  for the CS and Std-MIMO, respectively. In particular, we can observe that these values remain almost constant for all three cases, as predicted by the (2). The side-lobe discrepancies between simulations and measurements can be attributed to imperfections of the anechoic set-up, cf. Figure 5.

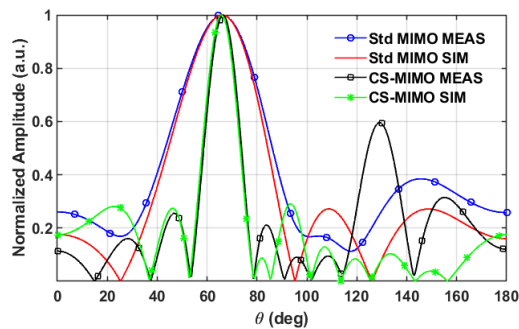
Finally, Figure 7 shows the processed radar images of the corner reflector placed in front of the radar. From these pictures, we can observe the improvement of the angular resolution obtained by the CS-MIMO, as well as a range resolution of 100 mm, consistent with the 1.5 GHz bandwidth of the radar signal. The two images reveal the presence of side lobes, already shown in Figure 6. These results therefore experimentally validated the assessment of Section 2, which describes the design degrees of freedom for a  $2 \times 2$  CS-MIMO antenna design, and demonstrated that the proposed design can effectively improve at least by a factor of 2.9 the angular resolution in millimeter-wave radar without raising the number of antennas compared to the  $2 \times 2$  Std-MIMO. Furthermore, field of view (FOV) is approximately maintained. It is worth noting that the FoV is still an open topic for CS MIMO antenna and it is beyond the scope of the present work.



(a) Corner reflector in  $\theta = 0$  deg.



(b) Corner reflector in  $\theta = 12$  deg.



(c) Corner reflector in  $\theta = 24$  deg.

**Figure 6.** Azimuthal response of both Std-MIMO and CS-MIMO for a corner reflector placed at 3.25 m, with different antenna-target relative orientations.

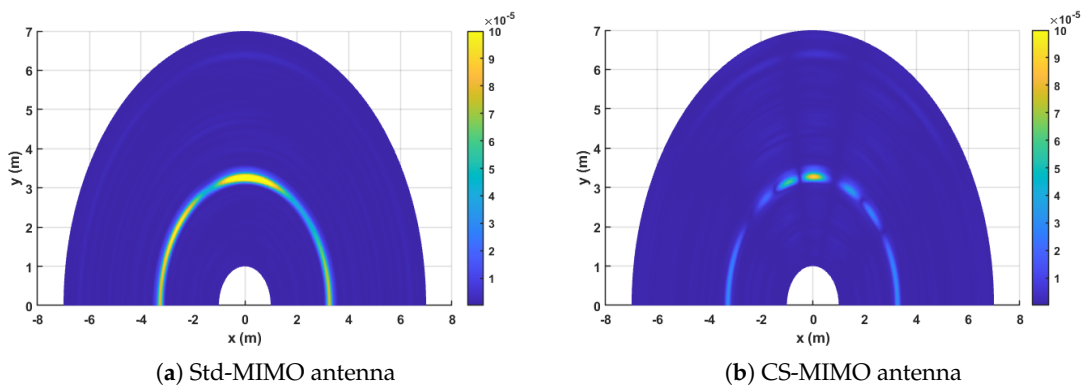


**Figure 7.** Radar images of a corner reflector placed in front of the MIMO radar.

## 5. Conclusions

This paper has dealt with the assessment and design of a novel patch MIMO antenna for millimeter-wave radar applications obtained exploiting the compressive sensing technique. It has analyzed all the possible configurations resulting from a  $2TX - 2RX$  channels case of study, in terms of both their compression ratio and angular resolution. We adopted the compression limit of 40% as resulted from previous studies to preserve the quality of the radar image, and according to this criterion, we selected one configuration among those available. On the other hand, investigating different CS configurations demonstrates that the same compression rate leads to the same angular resolution.

The antenna configuration was designed, fabricated and tested in a controlled environment. For a meaningful validation of the results, the radar image produced by the antenna under evaluation has been compared with the one achieved by a corresponding standard MIMO antenna. The comparison between simulations and experimental measurements, supports the validation.

The results presented in this paper demonstrate that the proper control of random sampling antenna positions can effectively improve the angular resolution by a factor of 2.9, with respect to a dense array based on Nyquist criteria, while needing significantly fewer elements. Furthermore, although the CS-MIMO performance depends on the view angle, its results are consistent with the Std-MIMO at different viewing angles.

Worth mentioning that the expected field of view in the context of CS, represents a feature to be investigated in future works, and at present, it is not possible to predict in general its value. In fact, it appears to be related to the basis function adopted in the CS technique, as well as to the specific random distribution of the antenna elements and thus it results to be not uniquely determined on the basis of the antenna elements distribution and aperture length.

As a final remark in this paper, for the first time, we demonstrated the effective capability of a CS-MIMO antenna operating at millimeter-wave to increase the angular resolution in radar applications. At the best of the author knowledge, it represents the first practical implementation of a complete antenna operating under these specifications, while maintaining constant the number of  $TX - RX$  radar front-end channels.

**Author Contributions:** N.R., G.C., and A.C. initiated and discussed the research problem; N.R. and M.L. performed experiments; N.R. and M.P. analyzed the data; N.R. and A.C. wrote the paper. All authors have read and agreed to the published version of the manuscript.

**Funding:** This work was partially funded by the National Italian Research Project, PRIN-2015 entitled “Millimetre-wave GaN-based radar system for early detection of micro unmanned aerial vehicles” grant number Prot. 2015CPC2MA, and partially by the Foundation Ente Cassa di Risparmio di Firenze under the grant number 2017-0941.

**Conflicts of Interest:** The authors declare no conflicts of interest.

## References

1. Hasch, J.; Topak, E.; Schnabel, R.; Zwick, T.; Weigel, R.; Waldschmidt, C. Millimeter-wave technology for automotive radar sensors in the 77 GHz frequency band. *IEEE Trans. Microw. Theory Tech.* **2012**, *60*, 845–860. [[CrossRef](#)]
2. Tarchi, D.; Oliveri, F.; Sammartino, P.F. MIMO radar and ground-based SAR imaging systems: Equivalent approaches for remote sensing. *IEEE Trans. Geosci. Remote Sens.* **2012**, *51*, 425–435. [[CrossRef](#)]
3. Cidronali, A.; Passafiume, M.; Colantonio, P.; Collodi, G.; Florian, C.; Leuzzi, G.; Pirola, M.; Ramella, C.; Santarelli, A.; Traverso, P. System Level Analysis of Millimetre-wave GaN-based MIMO Radar for Detection of Micro Unmanned Aerial Vehicles. In Proceedings of the 2019 PhotonIcs Electromagnetics Research Symposium—Spring (PIERS-Spring), Rome, Italy, 17–20 June 2019; pp. 438–450. [[CrossRef](#)]
4. Vasanelli, C.; Batra, R.; Di Serio, A.; Boegelsack, F.; Waldschmidt, C. Assessment of a millimeter-wave antenna system for MIMO radar applications. *IEEE Antennas Wirel. Propag. Lett.* **2016**, *16*, 1261–1264. [[CrossRef](#)]

5. Li, J.; Stoica, P. *MIMO Radar Signal Processing*; Wiley Online Library, John Wiley & Sons, Inc.: Hoboken, NJ, USA, 2009; Volume 7.
6. Bliss, D.; Forsythe, K. Multiple-input multiple-output (MIMO) radar and imaging: Degrees of freedom and resolution. In Proceedings of the Thirty-Seventh Asilomar Conference on Signals, Systems & Computers, Pacific Grove, CA, USA, 9–12 November 2003; Volume 1, pp. 54–59.
7. Ma, Y.; Miao, C.; Zhao, Y.; Wu, W. An MIMO radar system based on the sparse-array and its frequency migration calibration method. *Sensors* **2019**, *19*, 3580. [[CrossRef](#)]
8. Chen, Z.; Cao, Z.; He, X.; Jin, Y.; Li, J.; Chen, P. DoA and DoD Estimation and Hybrid Beamforming for Radar-Aided mmWave MIMO Vehicular Communication Systems. *Electronics* **2018**, *7*, 40. [[CrossRef](#)]
9. Donoho, D.L. Compressed sensing. *IEEE Trans. Inf. Theory* **2006**, *52*, 1289–1306. [[CrossRef](#)]
10. Yu, Y.; Petropulu, A.P.; Poor, H.V. MIMO radar using compressive sampling. *IEEE J. Sel. Top. Signal Process.* **2010**, *4*, 146–163. [[CrossRef](#)]
11. Rossi, M.; Haimovich, A.M.; Eldar, Y.C. Spatial compressive sensing for MIMO radar. *IEEE Trans. Signal Process.* **2013**, *62*, 419–430. [[CrossRef](#)]
12. Hu, S.; Shu, C.; Alfadhl, Y.; Chen, X. W Band Imaging System Using Linear Sparse Periodic Antenna Array and Compressive Sensing for Personnel Screening. *IEEE Access* **2019**, *7*, 173603–173611. [[CrossRef](#)]
13. Buttazzoni, G.; Babich, F.; Vatta, F.; Comisso, M. Geometrical Synthesis of Sparse Antenna Arrays Using Compressive Sensing for 5G IoT Applications. *Sensors* **2020**, *20*, 350. [[CrossRef](#)] [[PubMed](#)]
14. Pieraccini, M.; Rojhani, N.; Miccinesi, L. Compressive sensing for ground based synthetic aperture radar. *Remote Sens.* **2018**, *10*, 1960. [[CrossRef](#)]
15. Wimalajeewa, T.; Chen, H.; Varshney, P.K. Performance limits of compressive sensing-based signal classification. *IEEE Trans. Signal Process.* **2012**, *60*, 2758–2770. [[CrossRef](#)]
16. Hadi, M.A.; Alshebeili, S.; Jamil, K.; El-Samie, F.E.A. Compressive sensing applied to radar systems: An overview. *Signal Image Video Process.* **2015**, *9*, 25–39. [[CrossRef](#)]
17. Yu, Y.; Petropulu, A.P.; Poor, H.V. Measurement matrix design for compressive sensing-based MIMO radar. *IEEE Trans. Signal Process.* **2011**, *59*, 5338–5352.
18. Maddio, S.; Pelosi, G.; Righini, M.; Selleri, S. A Compact Series Array for Vehicular Communication in the C-Band. In Proceedings of the 2019 IEEE International Symposium on Antennas and Propagation and USNC-URSI Radio Science Meeting, Atlanta, GA, USA, 7–12 July 2019; pp. 1337–1338.
19. Garg, R.; Bhartia, P.; Bahl, I.J.; Ittipiboon, A. *Microstrip Antenna Design Handbook*; Artech House: Norwood, MA, USA, 2001.
20. Yuan, T.; Yuan, N.; Li, L.W. A novel series-fed taper antenna array design. *IEEE Antennas Wirel. Propag. Lett.* **2008**, *7*, 362–365. [[CrossRef](#)]
21. Abbasi Layegh, M.; Ghobadi, C.; Nourinia, J. The Optimization Design of a Novel Slotted Microstrip Patch Antenna with Multi-Bands Using Adaptive Network-Based Fuzzy Inference System. *Technologies* **2017**, *5*, 75. [[CrossRef](#)]
22. Brooker, G.M. Understanding millimetre wave FMCW radars. In Proceedings of the 1st international Conference on Sensing Technology, Palmerston North, New Zealand, 21–23 November 2005; pp. 152–157.
23. Maddio, S.; Cidronali, A.; Manes, G. Real-time adaptive transmitter leakage cancelling in 5.8-GHz full-duplex transceivers. *IEEE Trans. Microw. Theory Tech.* **2015**, *63*, 509–519. [[CrossRef](#)]

